

A PARAMETRIC STUDY OF THE REQUIRED SEATING LENGTH FOR BRIDGE DECKS DURING EARTHQUAKE

HONG HAO *

School of Civil and Structural Engineering, Nanyang Technological University, Nanyang Ave., Singapore 639798, Singapore

SUMMARY

During the recent major earthquakes, some bridges suffered severe damage due to the pull-off-and-drop collapse of their decks. This is due to the large differential movements of the adjacent spans of bridges during strong shaking compared to the seating lengths provided. The differential movements are primarily due to the different vibration properties of adjacent spans and non-uniform ground excitations at the bridge supports. This paper analyses the effects of various bridge and ground motion parameters on the required seating lengths for bridge decks to prevent the pull-off-and-drop collapse. The random vibration method is used in the analysis. A two-span bridge model with different span lengths and vibration frequencies and subjected to various spatially varying ground excitations is analysed. Non-uniform spatial ground motions are modelled by the filtered Tajimi–Kanai power spectral density function and an empirical coherency function. Ground motions with different intensities, different cross-correlations and different site conditions are considered in the study. The required seating lengths for bridge decks are calculated. Numerical results are presented and discussed with respect to different bridge vibration and ground motion properties. © 1998 John Wiley & Sons, Ltd.

Earthquake Engng. Struct. Dyn., **27**, 91–103 (1998)

KEY WORDS: spatial variation; differential movements; bridge deck ground displacement

INTRODUCTION

Pull-off-and-drop collapses of bridge decks were observed due to differential movements between adjacent bridge spans, in two recent major earthquakes. For example, the collapse of one panel of the San Francisco Bay Bridge during the October 17, 1989 Loma Prieta earthquake in California, and more recently, the collapse of the approach span of the Nishinomiya-Ko Bridge during the January 17, 1995 Hyogo-Ken Nanbu earthquake in Kobe, Japan, were caused by differential movements between adjacent spans. The collapses resulted in complete close down of the two bridges after the events.

The collapsed upper deck of the Bay Bridge was 50 ft (15.24 m) long, and was connected on its east end to another span with a series of connections that acted as pin joints. On the west end, however, the deck rested on a series of stiffened seat connections with no provisions for restraining the horizontal movement of the deck. During the earthquake, the east end moved eastward about 7 in (18 cm), while the seating length of the stiffened seat connection on the west end of the deck was only about 5 in (12.7 cm). The horizontal movement of the deck being larger than the seating length of the support, the deck was pulled off the support and dropped on the west end.¹ The approach span of the Nishinomiya-Ko Bridge was 52 m long, and was supported by seat connection on an elevated support. Adjacent to it on the west was a 252 m long tied arch main span. The vibration properties of the two adjacent spans differ considerably. The ground motions at the three supports also differ from each other significantly due to the large separation distance. Although the

* Correspondence to: Hong Hao, Senior Lecturer, School of Civil and Structural Engineering, Nanyang Technological University, Nanyang Avenue, Singapore 2263. E-mail: chhao@ntu.edu.sg

seating length provided for the dropped deck was about 0.8 m, the change in the vibration periods of the two adjacent spans and the pronounced spatial variations of ground excitations at different supports induced very significant differential movements of the two adjacent spans that resulted in the 52 m steel box girder approach span being pulled westward off the support and dropped.² The differential movements of bridge decks were also observed in other earthquakes, e.g. some pounding damage to decks was observed on bridges of freeway 5 in California during the Northridge earthquake.³

Long span structure response to non-uniform support excitations has been investigated recently by many authors.^{4–9} All of those studies concentrate on the response of a single structure with multiple supports and subjected to non-uniform multiple excitations. None of them specifically studied the differential movements of adjacent structures excited by correlated non-uniform ground motions. The present paper carries out a parametric study of the required seating length, which is the maximum differential movement of the adjacent bridge spans, for a bridge deck to prevent the pull-off-and-drop collapse. A two-span bridge model with different span lengths and vibration frequencies and subjected to different non-uniform support excitations is analysed. Random vibration method is used in the analysis. Non-uniform ground excitations with different intensities and spatial variations are considered in the analyses. They are modelled by the filtered Tajimi–Kanai¹⁰ power spectral density function and an empirical coherency loss function.¹¹ The effects of the site conditions and damping ratios on the required seating lengths are also studied. Numerical results are presented and discussed with respect to the various bridge and ground motion properties.

SPATIAL GROUND MOTION MODEL

With the stationarity assumption, the ground motion cross-power spectral density function can be modelled as

$$\begin{aligned} S_{kl}(\bar{\omega}) &= S_g(\bar{\omega})\gamma_{kl}(\bar{\omega}, d_{kl}) \\ &= |H_f(\bar{\omega})|^2 S_0(\bar{\omega}) |\gamma_{kl}(\bar{\omega}, d_{kl})| \exp(-i\bar{\omega}d_{kl}/v) \end{aligned} \quad (1)$$

where $\bar{\omega}$ is the circular frequency, v the apparent ground motion propagation velocity, d_{kl} the projected distance between points k and l on the ground surface in the ground motion propagation direction, and

$$|H_f(\bar{\omega})|^2 = \frac{\bar{\omega}^4}{(\omega_f^2 - \bar{\omega}^2)^2 + 4\xi_f^2\omega_f^2\bar{\omega}^2} \quad (2)$$

is a highpass filter with centre frequency ω_f and damping ratio ξ_f ,¹⁰ and

$$S_0(\bar{\omega}) = \frac{1 + 4\xi_g^2\bar{\omega}^2/\omega_g^2}{(1 - \bar{\omega}^2/\omega_g^2)^2 + 4\xi_g^2\omega^2/\omega_g^2} \Gamma \quad (3)$$

is the Tajimi–Kanai ground acceleration power spectral density function,¹² in which ω_g and ξ_g are the centre frequency and damping ratio, respectively, and both depend on the site conditions, epicentral distance and earthquake magnitude,¹³ and Γ is a scale factor depending on the ground motion intensity.

The factor $\exp(-i\bar{\omega}d_{kl}/v)$ in equation (1) represents the phase shift between the ground motions at points k and l ; and

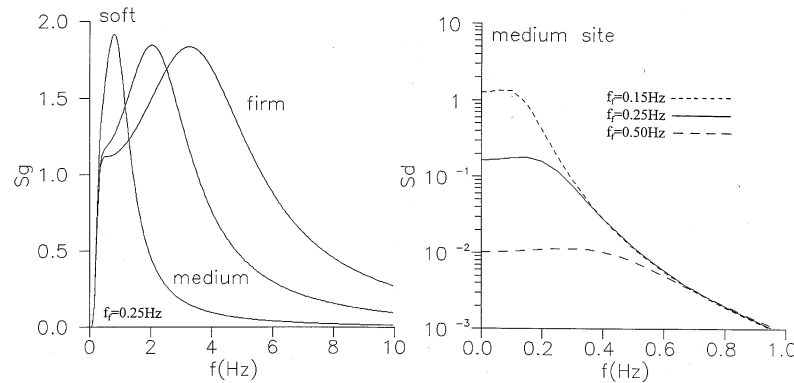
$$|\gamma_{kl}(\bar{\omega}, d_{kl})| = \exp(-\beta d_{kl}) \exp[-\alpha(\bar{\omega})\sqrt{d_{kl}}(\bar{\omega}/2\pi)^2] \quad (4)$$

is an empirical coherency loss function for ground motion propagating from points k to l ,¹¹ where

$$\alpha(\bar{\omega}) = \begin{cases} 2\pi a/\bar{\omega} + b\bar{\omega}/2\pi + c, & 0.314 \text{ rad/s} \leq \bar{\omega} \leq 62.83 \text{ rad/s} \\ 0.1a + 10b + c, & \bar{\omega} > 62.83 \text{ rad/s} \end{cases} \quad (5)$$

Table I. Central frequencies and damping ratios for the three sites

Site	f_g (Hz)	ξ_g
Firm	4.0	0.6
Medium firm	2.5	0.6
Soft	1.0	0.6

Figure 1. Ground acceleration and displacement power spectral density functions with respect to different site conditions and unit Γ

where a , b , c and β are constants which can be determined by a least-squares fit of equation (4) to the coherency loss of actually recorded motions.

In this study, three different site conditions representing firm, medium firm and soft sites are considered. The centre frequencies and damping ratios of the three sites are given in Table I. It should be noted that a constant ξ_g is used for all three site conditions since there is no reliable conclusion yet on how ξ_g varies with the site conditions. The corresponding power spectral density functions with a unit Γ and $f_f = \omega_f/2\pi = 0.25$ Hz and $\xi_f = 0.6$ are shown in Figure 1.

The highpass filter of equation (2) is applied in ground acceleration power spectral density function to filter out energy at zero and very low frequencies to correct the singularity in ground velocity and displacement power spectral density functions, and to prevent the drift of ground velocity and displacement. There is no solid physical base for the choice of the central frequency f_f and damping ratio ξ_f . Different authors used different values based on the nature of the problem. Figure 1 also shows the power spectral density functions of ground displacements ($S_g(\bar{\omega})/\bar{\omega}^4$) of the medium firm site conditions and different f_f . As can be seen, ground displacement power spectral density functions decrease drastically with the increase of the central frequency f_f .

Peak ground acceleration (PGA) and peak ground displacement (PGD) depend on the scale factor Γ . The relations between them and Γ can be established based on their respective power spectral density functions $S_g(\bar{\omega}) = |H_f(i\bar{\omega})|^2 S_0(\bar{\omega})$ and $S_g(\bar{\omega})/\bar{\omega}^4$ [see Appendix I]. Figure 2 shows PGA and PGD as functions of Γ for different site conditions. These results are obtained by assuming the ground motion duration $T = 20$ s, and a high cut-off frequency of 25 Hz. It should be noted that the first and the second spectral moments of $S_g(\bar{\omega})$ diverge if the upper limit of the integral in equation (21) is infinite [Appendix I]. Thus, only approximate spectral moments can be obtained by introducing a high cut-off frequency. In the present study, a high cut-off frequency of 25 Hz is used since it covers the dominant vibration frequencies of most engineering structures and earthquake ground motions. As can be seen, although the highpass filter has little effect on ground acceleration, it affects ground displacement significantly. A highpass filter with a lower centre frequency results in a larger PGD.

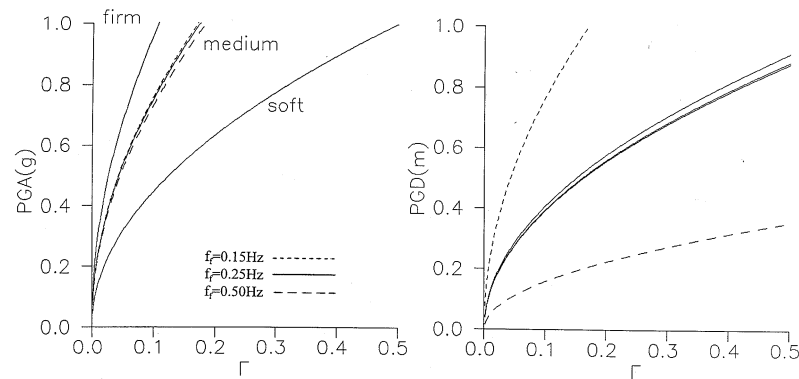


Figure 2. Peak ground acceleration and displacement corresponding to different site conditions and scale factor Γ

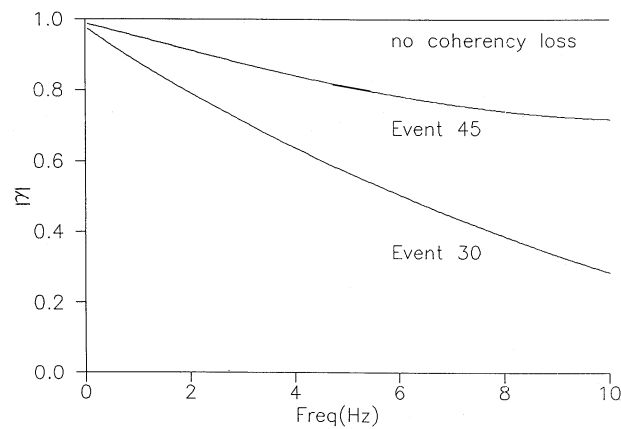


Figure 3. Three coherency loss functions with separation distance $d = 100$ m

Table II. Constants in coherency loss function

Event	$\beta (\times 10^{-4})$	$a (\times 10^{-4})$	$b (\times 10^{-4})$	$c (\times 10^{-4})$
30	2.25	106.6	0.265	-0.999
45	1.109	35.83	-0.181	1.177

Ground motion is assumed to propagate in the longitudinal direction of the bridge with an apparent velocity $v = 1000$ m/s in this study. Then, the distance d_{kl} between the two supports of each span equals the span length d . Constants in the coherency loss function used are those obtained from the recorded motions during Event 45 at the SMART-1 array.⁴ For comparison purposes, those corresponding to the recorded motions during Event 30 at the SMART-1 array, as well as the ground motions without coherency loss, i.e. $|\gamma_{kl}(i\omega, d_{kl})| = 1.0$, are also considered in the analyses. Table II gives the constants of the coherency loss function corresponding to the two events. Figure 3 shows the coherency loss functions estimated by equation (4) with $d_{kl} = 100$ m. As can be noted, recorded motions of Event 30 are less correlated than those of Event 45.

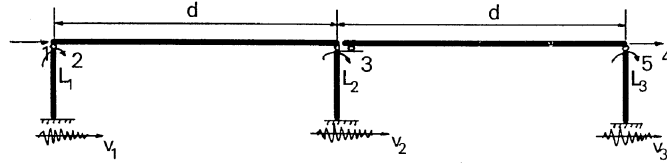


Figure 4. Two-span bridge model subjected to spatially varying ground excitations

BRIDGE MODEL AND EQUATIONS OF MOTION

A two-span bridge model is shown in Figure 4. The deck of the left span is pin connected at its two ends to the supports. The deck of the right span is pin connected only at its right end to the support and its left end is seat connected to the support without any lateral restraint. If one neglects the axial deformation of bridge deck and considers only the in-plane horizontal ground excitations in the analysis, the bridge model has five degrees of freedom (DOFs) and three support excitations as shown. The first three DOFs, which correspond to the left span, are independent of the DOFs 4 and 5 of the right span. The three support excitations are, however, cross correlated.

The total structural responses can be expressed as

$$\mathbf{U}^t = \mathbf{U} + \mathbf{U}^{qs} \quad (6)$$

where \mathbf{U} is the dynamic response vector and \mathbf{U}^{qs} is the quasi-static response vector. The dynamic responses can be calculated by solving the equation¹⁴

$$\mathbf{M}\ddot{\mathbf{U}} + \mathbf{C}\dot{\mathbf{U}} + \mathbf{K}_{ss}\mathbf{U} = \mathbf{M}\mathbf{K}_{ss}^{-1}\mathbf{K}_{sb}\ddot{\mathbf{V}}_g \quad (7)$$

and the quasi-static responses can be calculated by

$$\mathbf{U}^{qs} = -\mathbf{K}_{ss}^{-1}\mathbf{K}_{sb}\mathbf{V}_g \quad (8)$$

where \mathbf{M} is the mass matrix, \mathbf{C} the viscous damping matrix, \mathbf{K}_{ss} the stiffness matrix corresponding to the bridge response DOFs, and \mathbf{K}_{sb} the stiffness matrix corresponding to the coupled DOFs between the bridge responses and the support excitations. The subscripts 's' and 'b' refer to structure and base, respectively. $\mathbf{V}_g = (v_1, v_2, v_3)^T$ is the vector consisting of the three ground displacements at the three supports. The mass and stiffness matrices of the bridge model are given in Appendix II.

Since the dynamic responses of the two spans are independent of each other, they can be calculated separately. For the first span, it has

$$\mathbf{M}_1\ddot{\mathbf{U}}_1 + \mathbf{C}_1\dot{\mathbf{U}}_1 + \mathbf{K}_{s1}\mathbf{U}_1 = \mathbf{M}_1\mathbf{K}_{s1}^{-1}\mathbf{K}_{b1}\ddot{\mathbf{V}}_{g1} \quad (9)$$

where $\mathbf{V}_{g1} = (v_1, v_2)^T$. As the mass matrix \mathbf{M}_1 is a diagonal matrix with only one non-zero term associated with the lateral displacement of the first span (DOF 1), by neglecting the damping terms corresponding to the rotational DOFs, equation (9) can be reduced by static condensation to

$$m_1\ddot{u}_1 + c_{11}\dot{u}_1 + \frac{6k_1}{l_1^2}u_1 = \frac{m_1}{2}(\ddot{v}_1 + \ddot{v}_2) \quad (10)$$

where u_1 is the lateral displacement of the first span, which can be expressed in the frequency domain as

$$\bar{u}_1(i\bar{\omega}) = H_1(i\bar{\omega})(\bar{v}_1 + \bar{v}_2)/2 \quad (11)$$

and where $i = \sqrt{-1}$ is the imaginary unity, the bar over the quantity indicates the Fourier transform of the quantity, and

$$H_1(i\bar{\omega}) = \frac{1}{\omega_1^2 - \bar{\omega}^2 + 2i\xi_1\omega_1\bar{\omega}} \quad (12)$$

in which ξ_1 is the viscous damping ratio, $\omega_1 = \sqrt{6k_1/l_1^2 m_1}$ is the lateral vibration frequency of the first span.

Similarly, the lateral response of the second span u_4 in the frequency domain is

$$\bar{u}_4(i\bar{\omega}) = H_2(i\bar{\omega})\bar{v}_3 \quad (13)$$

where $H_2(i\bar{\omega})$ has a form similar to equation (12) except that ω_1 and ξ_1 are replaced by ω_2 and ξ_2 , and where $\omega_2 = \sqrt{3k_3/l_3^2 m_2}$ is the lateral vibration frequency of the second span.

The lateral quasi-static responses of the two spans can be derived as

$$u_1^{qs}(t) = \frac{1}{2}(v_1 + v_2) \quad (14)$$

$$u_4^{qs}(t) = v_3 \quad (15)$$

and hence, the total lateral responses of the two spans in the frequency domain are

$$\bar{u}_1^l(i\bar{\omega}) = H_1(i\bar{\omega})(\bar{v}_1 + \bar{v}_2)/2 + \frac{1}{2}(\bar{v}_1 + \bar{v}_2) \quad (16)$$

$$\bar{u}_4^l(i\bar{\omega}) = H_2(i\bar{\omega})\bar{v}_3 + \bar{v}_3 \quad (17)$$

The absolute value of the difference in lateral displacement between the two spans is given by

$$\bar{u}_s(i\bar{\omega}) = |\bar{u}_1^l(i\bar{\omega}) - \bar{u}_4^l(i\bar{\omega})| \quad (18)$$

and its power spectral density function can be derived as

$$\begin{aligned} S_{u_s}(\bar{\omega}) = & \left\{ \left[H_1 H_1^* / 2 - \frac{1}{\bar{\omega}^2} \text{real}(H_1) + \frac{1}{2\bar{\omega}^4} \right] \left[1 + |\gamma_{12}| \cos \frac{\bar{\omega} d_{12}^l}{v} \right] \right. \\ & + \left[H_2 H_2^* - \frac{2}{\bar{\omega}^2} \text{real}(H_2) + \frac{1}{\bar{\omega}^4} \right] - \left[\text{real}(H_1 H_2^*) - \frac{1}{\bar{\omega}^2} \text{real}(H_1) \right. \\ & \left. \left. - \frac{1}{\bar{\omega}^2} \text{real}(H_2) + \frac{1}{\bar{\omega}^4} \right] \left[|\gamma_{13}| \cos \frac{\bar{\omega} d_{13}^l}{v} + |\gamma_{23}| \cos \frac{\bar{\omega} d_{23}^l}{v} \right] \right\} S_g(\bar{\omega}) \end{aligned} \quad (19)$$

where ‘real’ represents the real part of a complex quantity, and ‘*’ the complex conjugate. If the ground excitations are spatially uniform, equation (19) is simplified to

$$S_{u_s}(\bar{\omega}) = [H_1 H_1^* + H_2 H_2^* - 2 \text{real}(H_1 H_2^*)] S_g(\bar{\omega}) \quad (20)$$

NUMERICAL RESULTS AND DISCUSSION

Let the viscous damping ratios of the two spans be both 5%. The required seating lengths for bridges to prevent the pull-off-and-drop collapse are calculated using the above derived power spectral density functions [Appendix I]. The effects of various parameters on required seating lengths are discussed.

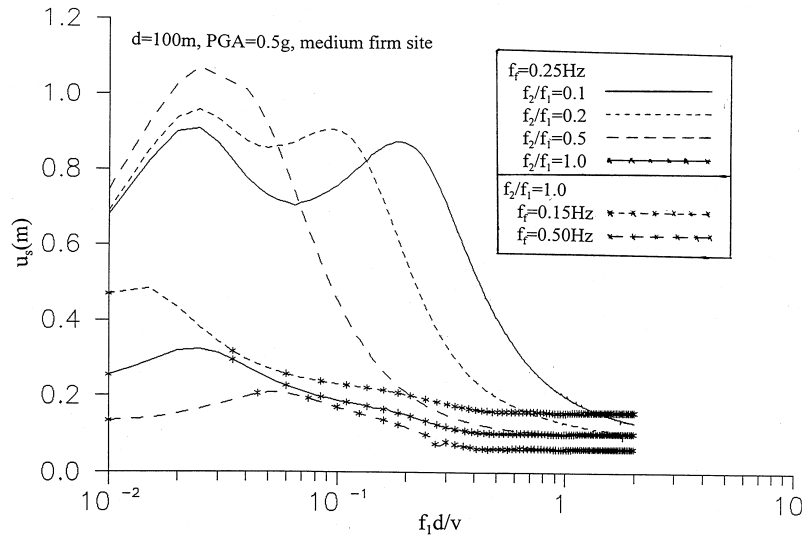


Figure 5. Required seating lengths of bridge spans obtained by varying bridge vibration frequencies

The effect of natural vibration frequency is studied first by calculating the required seating length of the bridge model with varying natural frequencies. Results for span length $d = 100$ m, coherency loss function of Event 45, $\text{PGA} = 0.5$ g, medium firm site conditions with $f_f = \omega_f/2\pi = 0.25$ Hz and $\xi_f = 0.6$, and different ratios of natural frequencies of the two spans, f_2/f_1 , are presented in Figure 5 with respect to the dimensionless parameter $f_1 d/v$, where $f_1 = \omega_1/2\pi$ is the natural frequency of the first span in Hertz. It is known that the in-phase and the out-of-phase excitations between ground motion phase shift (d/v) and structural vibration mode occur when $f d/v = 0.5(2n)$ and $f d/v = 0.5(2n - 1)$, respectively, where f is the vibration frequency of the structure and $n = 1, 2, \dots$; and the effect of multiple excitations is minimum when the phase shift of the multiple excitations is in-phase with the vibration mode, and maximum when they are out-of-phase.^{5,6,7,9}

As can be seen, the required seating length reaches the maximum value at $f_1 d/v = 0.025$ and 0.25 when $f_2/f_1 = 0.1$; at 0.025 and 0.125 when $f_2/f_1 = 0.2$; and at 0.025 when $f_2/f_1 = 1.0$, implying the maximum seating length is required when the natural frequency of the first or the second span coincides with the central frequency of the highpass filter, f_f . This observation indicates that the resonance of the first or the second span with the ground displacement causes the maximum differential movements. When $f_2/f_1 = 0.5$, however, only one peak occurs at $f_1 d/v = 0.034$, or $f_1 = 0.34$ Hz and $f_2 = 0.17$ Hz, i.e. when the natural frequencies of both spans are close to f_f . The above observations demonstrate that the displacement response depends strongly on the highpass filter because the quasi-static displacement depends on the ground displacement; and a lower centre frequency f_f of the highpass filter results in a larger ground displacement. Thus, the choice of the highpass filter, which is not based on any physical property of ground motion as discussed above, affects numerical results of displacement response significantly.

To further observe the effect of the highpass filter, numerical results corresponding to $f_f = 0.15$ and 0.5 Hz, $\xi_f = 0.6$ and $f_2/f_1 = 1.0$ are also shown in Figure 5. Significant difference between results obtained with different highpass filters is observed. As can be seen, displacement response increases with the ground displacement as the central frequency f_f of the highpass filter decreases.

The case of $f_2/f_1 = 0.5$ results in the largest peak value because both spans are resonant simultaneously with ground displacement as discussed above, whereas $f_2/f_1 = 1.0$ results in the smallest seating length requirement because the differential movements of the two spans are induced solely by non-uniform ground excitations. As $f_1 d/v$ increases, implying an f_1 increase, numerical values of all the cases approach a constant, which is

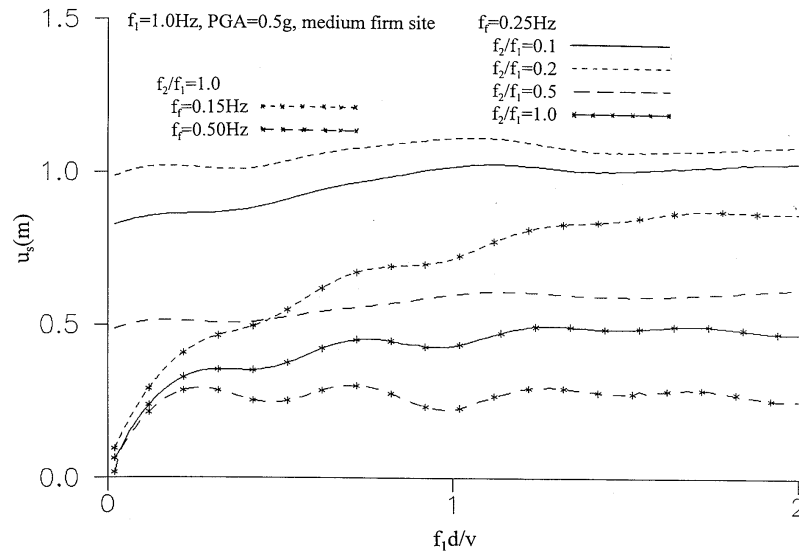


Figure 6. Required seating lengths of bridge spans obtained by varying span lengths

equal to the quasi-static response because dynamic response is very small at large vibration frequencies due to deamplification effect, but the quasi-static response is independent of the vibration frequency.

As the bridge span length affects the spatial variations of multiple support excitations, numerical results for the bridge model with $f_1 = 1.0$ Hz and different span lengths are calculated to analyse the ground motion spatial variation effect. Figure 6 shows those obtained with PGA = 0.5 g, medium firm site conditions, different natural frequency ratios, and different highpass filters. Generally, as can be noticed, the required seating length increases with $f_1 d/v$ or d , implying that less correlated ground motions cause larger differential displacement responses. This is because ground motions measured at points with a larger separation distance are less correlated, and less correlated motions cause larger quasi-static responses.⁴⁻⁹

The required seating lengths also oscillate with $f_1 d/v$. For the case of $f_2/f_1 = 1.0$, they reach the peak values at $f_1 d/v = 0.25, 0.75, 1.25$ and 1.75 , and the minimum values at $f_1 d/v = 0.5, 1.0, 1.5$ and 2.0 . This is because of the effects of in-phase and out-of-phase between the dominant ground motion phase shift and the fundamental vibration mode of the bridge. Since the separation distance between supports 1 and 3 is $2d = 200$ m, the out-of-phase excitations between the motions at supports 1 and 3 occur when $f_1 d/v = 0.25, 0.75, 1.25$ and 1.75 , whereas the in-phase excitations occur when $f_1 d/v = 0.5, 1.0, 1.5$ and 2.0 . The out-of-phase excitations cause the maximum differential displacements while the in-phase excitations produce the minimum differential displacements.

As can be seen in Figure 6 again, the highpass filter affects the differential displacement of adjacent bridge spans significantly. Since the choice of the central frequency f_f is not physically based, in the following discussion, all the numerical results are normalized by the corresponding peak ground displacement.

To study the relative importance of the various parameters of spatial ground motions and the vibration properties of the two adjacent bridge spans, Figure 7 shows the normalized relative displacements with respect to the frequency ratio f_2/f_1 obtained by using $f_1 = 0.5$ Hz and varying f_2 . As can be seen, the largest required seating length occurs when $f_2/f_1 = 0.5$, i.e. $f_2 = f_f = 0.25$ Hz, and the smallest seating length occurs when $f_2/f_1 = 1.0$. The ground motion spatial variation effect is most prominent when f_2/f_1 is close to unity, i.e. when the two adjacent spans have similar vibration properties. The less correlated ground motions (Event 30) cause larger differential displacements than the more correlated motions (Event 45). The ground motion spatial variation effect is, however, not pronounced if the vibration frequencies of the two spans differ significantly;

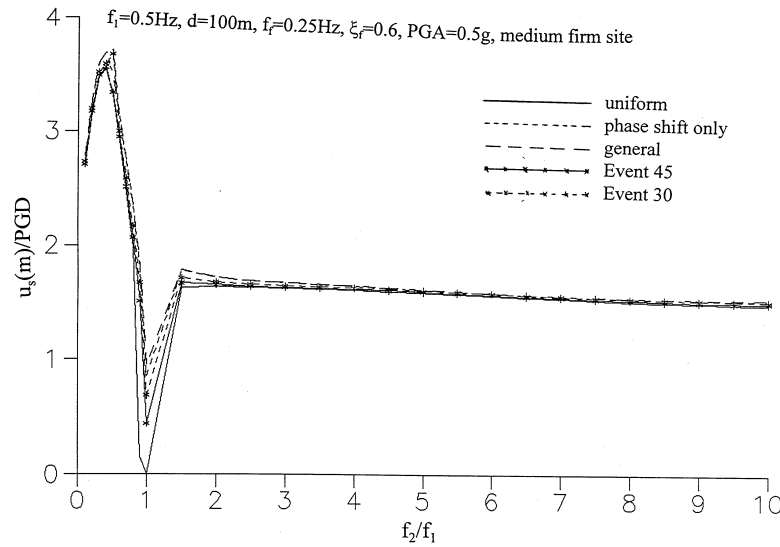


Figure 7. Normalized seating lengths for bridges subjected to multiple ground excitations with different spatial variations

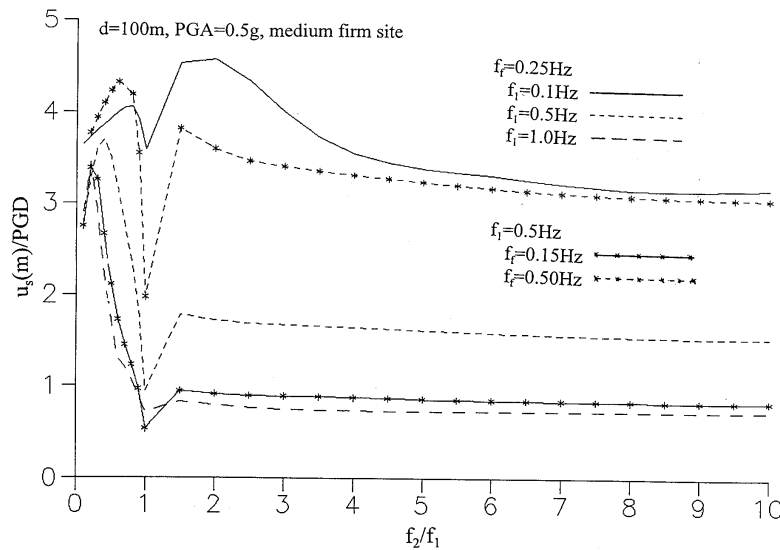


Figure 8. Normalized seating lengths for bridges having different natural frequencies

the dominant factor of causing the differential displacements is now the different vibration phases of the two spans. When f_2/f_1 is larger than 2.0, the required seating length approaches a constant, implying that the response of the second span is primarily caused by quasi-static response, which is independent of f_2 .

Figures 8 and 9 show the required seating lengths calculated by using different f_1 , different viscous damping ratios, and different site conditions. Besides the above observations, it can be seen that the natural vibration frequency of the bridge affects the required seating length significantly. The largest seating length is needed if the bridge resonates with the ground displacement.

The required seating length for bridge deck also depends on the damping ratios and ground motion intensities. Increase of the viscous damping is a very effective way to reduce the required seating length. As shown

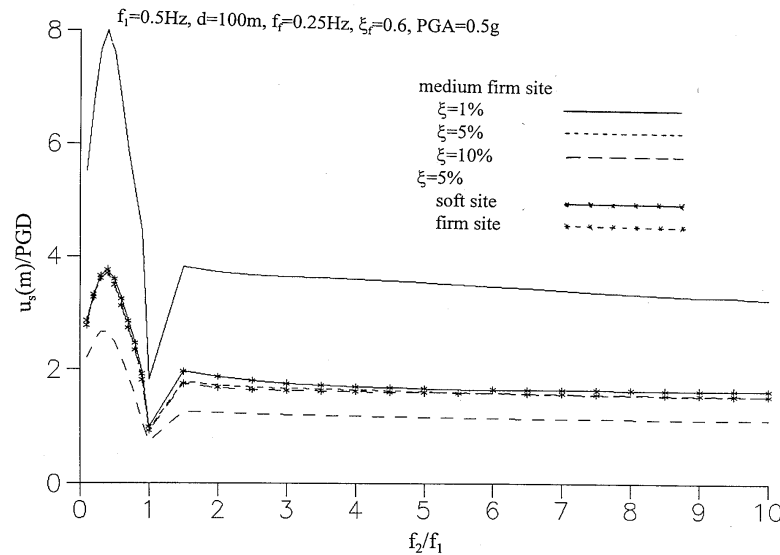


Figure 9. Normalized seating lengths for bridges having different damping ratios and on sites of different conditions

in Figure 9, the required seating length is reduced by more than 50 per cent by increasing the damping ratio from 1 to 5 per cent.

Also shown in Figure 9 are the normalized results corresponding to different site conditions. As can be seen, the normalized results for the three site conditions are very close to each other, implying a larger seating length should be provided for a bridge on a soft site than on a firm site. This is because the PGD corresponding to a soft site is larger than that corresponding to a firm site if the PGA for both sites are the same. Required seating lengths corresponding to different PGA are also calculated. It is interesting to note that the normalized relative displacements obtained by ground motions with different PGA are the same, indicating that the relative displacement and PGD are linearly proportional to each other although they are non-linearly proportional to PGA or Γ .

The above results demonstrated that bridge vibration properties, viscous damping ratios and spatial ground motions affect the differential responses of structures. Depending on the bridge vibration frequency, damping ratio, PGA and PGD, and site conditions, the seating length required to prevent the bridge deck being pulled off its support during a major earthquake could be more than 1.0 m. Because of the quasi-static response, the differential displacements strongly depend on ground displacement. In practice, most of the available ground motion information is ground accelerations, and ground displacements are usually obtained by numerically integrating the recorded ground accelerations. Mathematically, a highpass filter has to be applied to ground acceleration before integration to prevent ground velocity and displacement to drift from the zero axis. Since the choice of the highpass filter, especially the choice of the central frequency of the highpass filter, affects ground displacement substantially, it is crucial to find a reliable and physically meaningful central frequency for the highpass filter if ground motion spatial variation is considered in the structural response analysis.

CONCLUSIONS

The required seating lengths for bridge seat connections to prevent the pull-off-and-drop collapse during strong earthquakes have been calculated. The numerical results of the required seating lengths have been presented

and discussed with respect to the bridge vibration frequencies, span lengths, damping ratios, and the spatial ground excitations. It is found that:

1. The differential movements of bridge spans strongly depend on ground displacement. The largest seating length is required when the natural frequency of the bridge coincides with the central frequency of the ground displacement;
2. A larger seating length is required if multiple ground motions are less correlated; and if the multiple ground motion phase shift is out-of-phase with the fundamental bridge vibration mode;
3. The variation of vibration properties of two adjacent spans is the dominant factor causing differential displacements when the natural frequencies of the two spans differ from each other noticeably. However, ground motion spatial variations become the primary factor to cause differential displacements when the natural frequencies of the two spans are close to each other;
4. Damping ratios, site conditions and ground motion intensities all affect the required seating length. It is a very effective way to reduce the required seating length by increasing the damping of the bridge.

APPENDIX I

For a zero mean stationary process $x(t)$ with power spectral density function $S(\bar{\omega})$, its m th order spectral moment is defined as

$$\lambda_m = \int_0^\infty \bar{\omega}^m S(\bar{\omega}) d\bar{\omega} \quad (21)$$

In engineering applications, the spectral moment can be approximately calculated by

$$\lambda_m \approx \int_0^{\omega_c} \bar{\omega}^m S(\bar{\omega}) d\bar{\omega} \quad (22)$$

where ω_c is a high cut-off frequency.

The zero mean cross rate ν and the shape factor of the power spectral density δ can be obtained by

$$\nu = \frac{1}{\pi} \sqrt{\frac{\lambda_2}{\lambda_0}} \quad (23)$$

$$\delta = \sqrt{1 - \lambda_1^2 / \lambda_0 \lambda_2} \quad (24)$$

The mean peak response is then obtained by¹⁵

$$\bar{x}_{\max} = \left(\sqrt{2 \ln \nu_e T} + \frac{0.5772}{\sqrt{2 \ln \nu_e T}} \right) \sigma \quad (25)$$

where T is the duration of the stationary process, $\sigma = \sqrt{\lambda_0}$ is the standard deviation of the process, and

$$\nu_e T = \begin{cases} \max(2.1, 2\delta T), & 0 \leq \delta < 0.1 \\ (1.63\delta^{0.45} - 0.38)\nu T, & 0.1 \leq \delta < 0.69 \\ \nu T, & \delta \geq 0.69 \end{cases} \quad (26)$$

In this study, all the above integrations are carried out numerically by using the commercial mathematical library NAG.¹⁶

APPENDIX II

For the bridge model shown in Figure 4, the mass matrix is

$$\mathbf{M} = \begin{pmatrix} \begin{pmatrix} m_1 & 0 & 0 \\ 0 & 0 & 0 \\ 0 & 0 & 0 \end{pmatrix} & \mathbf{0} \\ \mathbf{0} & \begin{pmatrix} m_2 & 0 \\ 0 & 0 \end{pmatrix} \end{pmatrix} = \begin{pmatrix} \mathbf{M}_1 & \mathbf{0} \\ \mathbf{0} & \mathbf{M}_2 \end{pmatrix} \quad (27)$$

where m_1 and m_2 are the lumped masses of the two spans to their respective lateral displacement DOFs.

The stiffness matrices can be formed as

$$\mathbf{K}_{ss} = \begin{pmatrix} \begin{pmatrix} \frac{12k_1}{l_1^2} + \frac{12k_2}{l_2^2} & \frac{6k_1}{l_1} & \frac{6k_2}{l_2} \\ \frac{6k_1}{l_1} & 4k_1 & 0 \\ \frac{6k_2}{l_2} & 0 & 4k_2 \end{pmatrix} & \mathbf{0} \\ \mathbf{0} & \begin{pmatrix} \frac{12k_3}{l_3^2} & \frac{6k_3}{l_3} \\ \frac{6k_3}{l_3} & 4k_3 \end{pmatrix} \end{pmatrix} = \begin{pmatrix} \mathbf{K}_{s1} & \mathbf{0} \\ \mathbf{0} & \mathbf{K}_{s2} \end{pmatrix} \quad (28)$$

and

$$\mathbf{K}_{sb} = \begin{pmatrix} \begin{pmatrix} -\frac{12k_1}{l_1^2} & -\frac{12k_2}{l_2^2} \\ -\frac{6k_1}{l_1} & 0 \\ 0 & -\frac{6k_2}{l_2} \end{pmatrix} & \mathbf{0} \\ \mathbf{0} & \begin{pmatrix} -\frac{12k_3}{l_3^2} & -\frac{6k_3}{l_3} \\ -\frac{6k_3}{l_3} & 0 \end{pmatrix} \end{pmatrix} = \begin{pmatrix} \mathbf{K}_{b1} & \mathbf{0} \\ \mathbf{0} & \mathbf{K}_{b2} \end{pmatrix} \quad (29)$$

where $k_i = (EI)_i/l_i$, in which $(EI)_i$ and l_i are the flexural rigidity and the height of the i th support.

If $l_1 = l_2$ and $k_1 = k_2$, i.e. the first two supports of the left span are identical as they are assumed in this study, we set

$$\mathbf{K}_{ss}^{-1} \mathbf{K}_{sb} = \begin{pmatrix} -0.5 & -0.5 & 0 \\ -3/4l_1 & 3/4l_1 & 0 \\ 3/4l_1 & -3/4l_1 & 0 \\ 0 & 0 & -1 \\ 0 & 0 & 0 \end{pmatrix} \quad (30)$$

REFERENCES

1. A. Astaneh, 'Initial observations of the damage to the San Francisco Bay Bridge', in *Preliminary Report on the Seismological and Engineering Aspects of the October 17, 1989 Santa Cruz (Loma Prieta) Earthquake*, Report No. UCB/EERC-89/14, Chapter 4. Earthquake Engineering Research Center, University of California at Berkeley, 1989.
2. R. Park *et al.*, 'The Hyogo-Ken Nambu earthquake of 17 January 1995', *Bull. New Zealand Nat. Soc. Earthquake Engng.*, **28** (1) (Special Issue) (1995).
3. J. A. Norton *et al.*, 'Northridge Earthquake Reconnaissance Report', *Bull. New Zealand Nat. Soc. Earthquake Engng.*, **27** (4) (Special Issue) (1994).
4. H. Hao, 'Effects of spatial variation of ground motions on large multiply-supported structures', Report No. UCB/EERC-89/07, Earthquake Engng. Research Center, Univ. of California at Berkeley, 1989.
5. R. S. Harichandran and W. Wang, 'Response of indeterminate two-span beam to spatially varying seismic excitation', *Earthquake Engng. Struct. Dyn.*, **19**, 173–187 (1990).
6. A. Zerva, 'Response of multi-span beams to spatially incoherent seismic ground motions', *Earthquake Engng. Struct. Dyn.*, **19**, 819–832 (1990).

7. A. Der Kiureghian and A. Neuenhofer, 'A response spectrum method for multiple-support seismic excitations', *Report No. UCB/EERC-91/08*, Earthquake Engng. Research Center, Univ. of California at Berkeley, 1991.
8. M. Berrah and E. Kausel, 'Response spectrum analysis of structures subjected to spatially varying motions', *Earthquake Engng. Struct. Dyn.*, **21**, 461–470 (1992).
9. H. Hao, 'Arch responses to correlated multiple excitations', *Earthquake Engng. Struct. Dyn.*, **22**, 389–404 (1993).
10. P. Ruiz and J. Penzien, 'Probabilistic study of the behaviour of structures during earthquakes', *Report No. UCB/EERC-69/03*, Earthquake Engng. Research Center, Univ. of California at Berkeley, 1969.
11. H. Hao, C. S. Oliveira and J. Penzien, 'Multiple-station. ground motion processing and simulation based on SMART-1 array data', *Nucl. Engng. Des.*, **111**, 293–310 (1989).
12. H. Tajimi, 'A statistical method of determining the maximum response of a building structure during an earthquake', *Proc. 2nd World Conf. on Earthquake Engineering*, **2**, Tokyo, 1960.
13. S. S. Lai, 'Statistical characterization of strong ground motion using power spectral density function', *Bull. Seismic Soc. America*, **72**, 259–276 (1982).
14. R. W. Clough and J. Penzien, *Dynamics of Structures*, 2nd edn., McGraw-Hill, New York, 1993.
15. A. Der Kiureghian, 'Structural response to stationary excitation', *J. engng. mech. ASCE*, **106**, 1195–1213 (1980).
16. *The NAG Fortran Library Manual*, The Numerical Algorithms Group Limited, Wilkinson House, Jordan Hill Road, Oxford, UK OX2 8DR, July 1988.